DOI: 10.1002/ejic.200500881

Counteranion-Induced Formation of *cis* and *trans* Singly and Doubly H_2biim-Bridged Di-, Hexa-, and Polymeric Ag–H_2biim Complexes

Rui-Li Sang[a] and Li Xu*[a]

Keywords: Crystal engineering / Luminescence / Metal–metal interactions / N ligands / Silver

A series of *cis* and *trans* singly and doubly H_2biim-bridged di-, hexa-, and polymeric complexes of silver(I) (H_2biim = 2,2′-biimidazole), namely $[Ag_2(\mu\text{-}H_2biim)_2]SO_4\cdot 2H_2O$ (**1**), $[Ag_2(\mu\text{-}H_2biim)_2(\mu\text{-ox})]_n$ (**2**), $[Ag_6(\mu\text{-}H_2biim)_5(H_2biim)_2](ClO_4)_4(CH_3CO_2)_2\cdot 2H_2O$ (**3**), and $[Ag(\mu\text{-}H_2biim)(nicotinate)]_n$ (**4**) have been synthesized and characterized by X-ray crystallography and IR and photoluminescence spectroscopy. The structural topology of the Ag–H_2biim system is determined by the charge of the counteranions. Thus, dianionic counterions facilitate the formation of dimeric structures driven by the charge-balance requirement, whereas a monoanionic counterion favors the formation of helical structures. Counteranions of larger size lead to either finite helical structures or a *trans* arrangement of the coordinating nitrogen atoms because of steric requirements. Organic counteranions with a strong coordination ability bind to the Ag^+ ions while inorganic counteranions are uncoordinated. The argentophilic attraction is not dominant in this system. Examination of the luminescent properties of H_2biim and compounds **1**–**4** indicates that the fluorescence emission of H_2biim is effectively shifted upon metal coordination.

Introduction

The substitution reaction is one of the most important chemical reactions and is widely employed in the preparation of new chemical materials, especially supramolecular polymer materials. The general strategy is to use multifunctional organic ligands to replace inorganic ligands of simple starting metal complexes to build functional supramolecular architectures.[1–3] Crystal formation depends on many factors, including metal–ligand, metal–metal, ligand–ligands, hydrogen bonding, and π stacking interactions. Covalent metal–ligand interactions are the strongest and thus dominate crystal formation. Interactions between open metal ions, known as metal–metal bonds, are comparable in strength to metal–ligand bonds and are the driving force in the formation of metal clusters. However, interactions between closed metal ions, typically coinage ones, which are intermetallic attraction in nature,[4,5] are comparable to hydrogen bonds in strength. Thus, the aggregation of closed metal ions is flexible and depends on other factors, such as weak interactions and charge balance. Although metal coordination requirements are dominant in the global architecture, other auxiliary factors such as charge balance and weak, noncovalent requirements play a significant role due to the multiple bonding modes of the ligand and the variety of geometries available for some metal ions. Many metal complexes, especially those with neutral ligands, appear as cationic species and thus anionic counterparts are usually present for charge balance. The role of these counteranions has been the subject of several reports.[6–8] Recent research results have indicated that the coordinating ability, shape, and size of counteranions have a significant influence on the global structures through either metal coordination or crystal-packing effects when noncoordinated.[7,8] In the present work, we will describe the Ag–H_2biim system with various counteranions of different charge, size, and coordinating ability to compare their competitive power. Ag^+ is an appropriate probe as it has varied coordination geometries and is able to aggregate through argentophilic attractions.[6,7] 2,2′-Biimidazole is an evergreen ligand that has attracted constant interest in supramolecular chemistry,[9] biochemistry,[10] cluster science,[11] and antitumor drugs.[12] The Ag–H_2biim system is able to adopt multiple coordinating modes and a variety of geometries, and can thus serve as a probe to examine the role of the above counteranion characteristics in crystal-structure formation. Four new supramolecular complexes, namely $[Ag_2(\mu\text{-}H_2biim)_2]SO_4\cdot 2H_2O$ (**1**), $[Ag_2(\mu\text{-}H_2biim)_2(\mu\text{-ox})]_n$ (**2**), $[Ag_6(\mu\text{-}H_2biim)_5(H_2biim)_2](ClO_4)_4(CH_3CO_2)_2\cdot 4H_2O$ (**3**), and $[Ag(\mu\text{-}H_2biim)(nicotinate)]_n$ (**4**) have been synthesized and characterized and the influences of the competing counteranion characteristics (charge, coordinating ability, and size) in the crystal-structure formation will be discussed.

[a] State Key Laboratory of Structural Chemistry, Fujian Institute of Research on the Structure of Matter, Chinese Academy of Science,
Fuzhou, Fujian, 350002, China
Fax: +86-591-8370-5045
E-mail: xli@fjirsm.ac.cn

Results and Discussion

Syntheses of the Complexes

The syntheses of complexes **1**–**4** are summarized in Scheme 1. It is obvious that the complexation of Ag^+ and H_2biim depends on the charge, size, and coordination ability of the counteranions: organic counteranions of strong coordination ability, such as oxalate and nicotinate, become coordinated to produce the neutral reaction products **2** and **4**, whereas inorganic counteranions, such as ClO_4^{2-} and SO_4^{2-}, are uncoordinated, yielding charged, polynuclear Ag–H_2biim complexes. It seems that dianionic counterions facilitate the formation of dimeric structures, presumably as a consequence of the charge-balance requirement, as suggested by the formation of the dimers **1** and **2**. In contrast, monoanionic counterions tend to favor the formation of helical structures, as suggested by **3**, **4**, and the previously reported complex $[Ag(\mu\text{-}H_2biim)]NO_3$.[10b] The use of larger ClO_4^- instead of NO_3^- leads to the formation of the finite helical complex **3**.

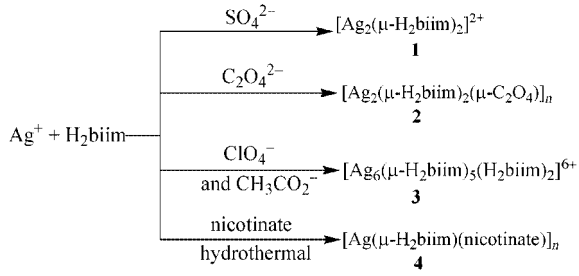

Scheme 1. Syntheses of compounds **1**–**4**.

Crystal Structures

$[Ag_2(\mu\text{-}H_2biim)_2]SO_4{\cdot}2H_2O$ (1)

The structure of the dicationic dimer of **1** is given in Figure 1 (a). The two Ag atoms are doubly bridged by H_2biim, forming a dicationic dimeric structure. Such a dimeric structure facilitates the charge balance through an alternating arrangement of the dimer and SO_4^{2-} in the resulting infinite chain (Figure 1, b). Each Ag^+ ion is coordinated to the two nitrogen atoms from the different H_2biim moieties [Ag–N1 = 2.149(6), Ag–N3 = 2.130(5) Å] in an almost linear arrangement [N1–Ag–N3 = 170.6(2)°] as in the case of $[\{Ru(pap)_2(Biim)\}_2Ag_2](ClO_4)_2$ (179°)[5a] and $[Ag_2(napy)_2](ClO_4)_2$ (168°).[5d] The distance between the two Ag atoms is 2.818(1) Å, slightly shorter than in the doubly bridged $[\{Ru(pap)_2(Biim)\}_2Ag_2](ClO_4)_2$ [2.890(2) Å],[5a] $[Ag_2(dpim)_2(CH_3CN)_2](ClO_4)_2$ [2.9932(9) Å],[5b] and $[Ag_2(Ph_2PCH_2SPh)_2](ClO_4)_2$ [2.9501(8) and 2.9732(9) Å][5c] but comparable to that in $[Ag_2(napy)_2](ClO_4)_2$[5d] [2.748(2) Å]. The H_2biim ligands are slightly twisted, with a dihedral angle of 14.6°. The two biimidazole ligands are nearly perpendicular to each other (the angle between their least-squares planes is 77.1°). The two neighboring $[Ag_2(H_2biim)_2]^{2+}$ units are linked together by weak Ag···$O_{sulfate}$ interactions into a one-dimensional chain with a pitch of 10.32 Å running along the *c* axis (Figure 1, b).

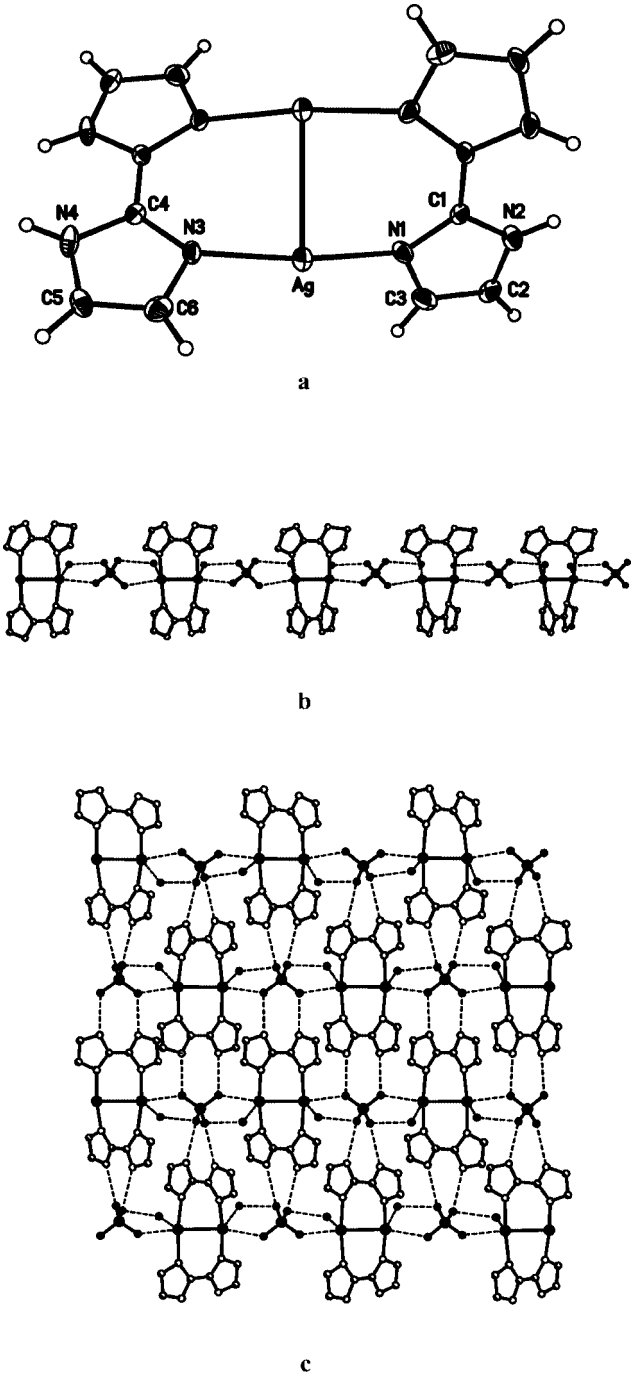

Figure 1. (a) ORTEP drawing of the $[Ag_2(H_2biim)_2]^{2+}$ moiety of **1** with 30% probability thermal ellipsoids. (b) Infinite chain showing Ag^+–SO_4^{2-} and Ag^+–H_2O interactions. (c) Hydrogen-bonded sheet structure.

The water molecules interact weakly with the Ag atoms [2.756(2) Å] and sulfate (2.861 Å). The staggered arrangement of H_2biim of the neighboring chains allows for the formation of interchain N–H_{biim}···$O_{sulfate}$ hydrogen bonds (N4···O1 = 2.722, N2···O2 = 2.770 Å) in the resultant sheet structure, as shown in part c of Figure 1.

[Ag$_2$(μ-H$_2$biim)$_2$(μ-ox)] (2)

As shown in part a of Figure 2, compound **2** has a similar, doubly bridged dimeric structure to that of **1** although their counteranions are remarkably different in size, shape, and coordinating ability, thus indicating that the dimeric structure results from the charge, rather than the other characteristics such as coordinating ability, size, and shape, of the counteranions. Different from the inorganic counteranion SO_4^{2-}, the organic counteranion oxalate coordinates more strongly and acts as a didentate bridging ligand to link the dimers into an infinite chain [Ag–O_{ox} = 2.392(4) Å; Figure 2, b]. The Ag–Ag separation [2.8437(9) Å] is not significantly changed by the oxalate coordination. Nevertheless, the binding of oxalate to Ag^+ apparently changes the geometric parameters of the dimer, as indicated by the considerably smaller N–Ag–N angle [132.95(16)°] and longer Ag–N distances [2.236(4) and 2.203(4) Å] than those in **1**.

Additionally, the direct coordination of oxalate also accounts for the absence of lattice water molecules in the crystals. The H_2biim ligands are slightly twisted, and their dihedral angle of 28.2° is larger than that (14.6°) in **1**. As opposed to **1**, the least-squares planes of the two biimidazole ligands are nearly parallel to each other. The atoms Ag, N1, N3, and O1 are nearly coplanar. In spite of these changes, the crystal structures of **1** and **2** are somewhat similar to each other: both have a one-dimensional, chain-like structure formed by either Ag–O_{ox} bonds or Ag···$O_{sulfate}$ interactions and hydrogen-bonded sheet structures due to interchain N–H···$O_{sulfate}$ or N–H···O_{ox} (2.722, 2.746 Å) hydrogen bonds, as indicated in Figures 1 (c) and 2 (b), respectively.

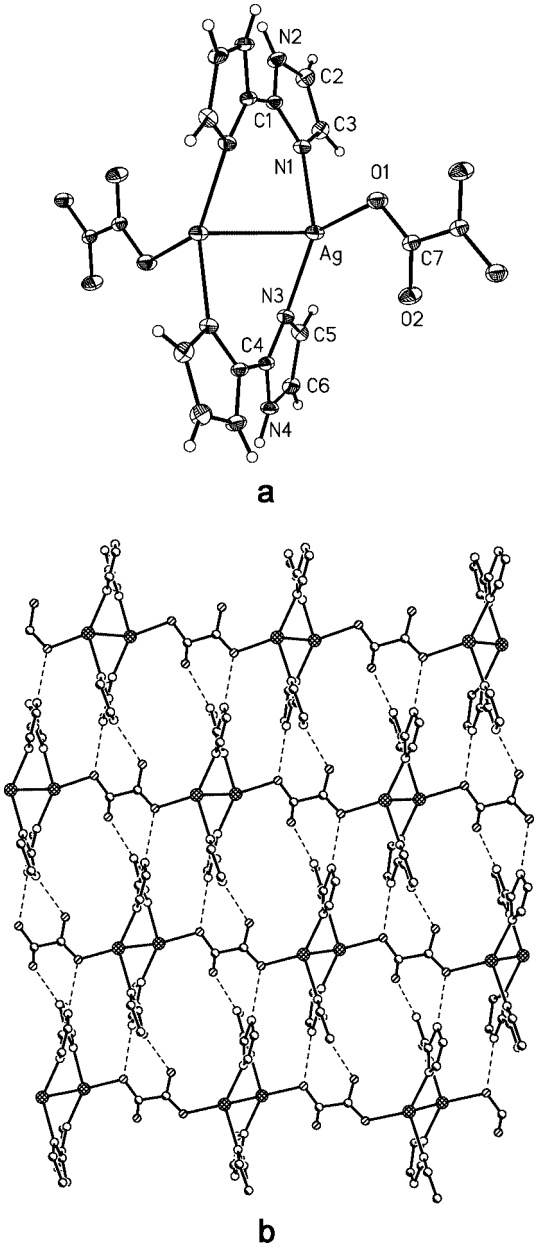

Figure 2. (a) ORTEP drawing of **2** with 30% probability thermal ellipsoids. (b) Sheet structure showing interchain $C_2O_4^{2-}$···H_2biim hydrogen bonds.

[Ag$_6$(μ-$_2$biim)$_5$(H$_2$biim)$_2$](ClO$_4$)$_4$(CH$_3$CO$_2$)$_2$·4H$_2$O (3)

Complex **3** contains a mixture of monoanionic inorganic and organic anions and consequently adopts the hexanuclear helical structure $[Ag_6(\mu\text{-}H_2biim)_5(H_2biim)_2]^{6+}$, as shown in Figure 3 (a), instead of a dimeric structure, similar

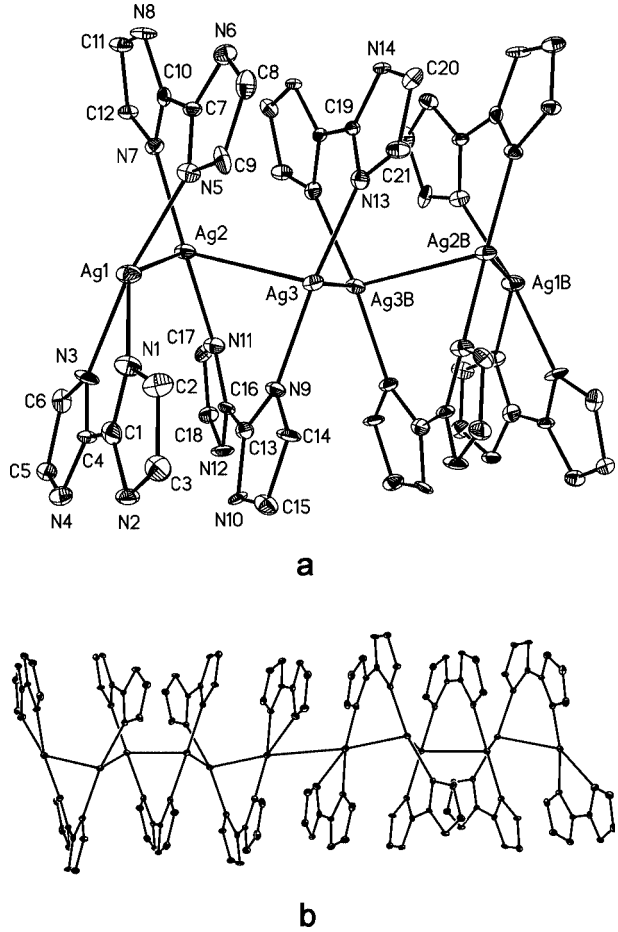

Figure 3. (a) ORTEP drawing of $[Ag_6(\mu\text{-}H_2biim)_5(H_2biim)_2]^{6+}$(**3**). (b) 1D Ag chain.

to that reported for [Ag(H_2biim)NO_3].[10b] In this helical structure, the counteranion lies alongside the Ag^+ chain[10b] rather than between the Ag^+ ions to facilitate the charge balance. The hexameric structure has C_2 symmetry, with the twofold axis bisecting the Ag3–Ag3a bond. As opposed to **1** and **2**, the neighboring Ag^+ in **3** is singly bridged by the five H_2biim ligands through the *cis* nitrogen atoms, yielding a hexameric helix with Ag–N bonds ranging from 2.112(2) to 2.157(2) Å. The middle Ag^+ atoms (Ag2, Ag3) have an almost linear coordination geometry [N–Ag–N = 164.8(2)° and 172.6(2)°] that is stabilized by Ag···$O_{perchlorate}$ interactions (Ag2···O = 2.912, Ag3···O = 2.879 Å). The helix ends at Ag1 as it is chelated by H_2biim. It is notable that the Ag1–N1 distance of 2.543(7) Å is comparable to the above Ag···$O_{perchlorate}$ separations but considerably longer than the Ag1–N3 bond [2.163(5) Å], and is responsible for the almost linear N3–Ag1–N5 angle [170.4(2)°]. The Ag–Ag distances [Ag1–Ag2 = 2.9335(18), Ag2–Ag3 = 3.0093(16), Ag3–Ag3′ = 3.078(2) Å] are significantly longer than in **1** and **2** but similar to those reported previously.[10,11] Compound **3** adopts a hexameric helical structure rather than an infinite helical structure similar to the reported nitrate derivative[10b] as a consequence of the chelating instead of bridging H_2biim ligands that terminate the growth of the helix. This observation may be attributed to the steric requirement of perchlorate, which is larger than the nitrate in 1D [Ag(μ-H_2biim)]NO_3,[10b] and is thus unable to allow for the presence of counteranions surrounding the terminal Ag atoms (Ag1). This leads to the structural evolution whereby two sevenths of the bridging H_2biim ligands in the one-dimensional helical [Ag(μ-H_2biim)]NO_3[10b] become chelated in the present hexanuclear compound to compensate for the missing Ag1–O interaction that is needed to stabilize the linear coordination. The acetate groups are involved in hydrogen bonding with H_2biim (2.7–2.8 Å) and water (2.79 Å) rather than with the Ag atoms.

The preference of carboxylate groups to form hydrogen bonds with H_2biim rather than coordinate to metal ions has been demonstrated in the complexes [$M(H_2biim)_2(H_2O)_2$]-$(RCO_2)_2$.[9f] The chelating H_2biim is twisted to a lesser extent (the dihedral angle is 10.8°) than the bridging ones (22–25°). The helix is also characteristic of an approximately parallel arrangement of neighboring H_2biim ligands, with the dihedral angles and the distances between the ring atoms and the least-square planes ranging from 8–12° and 2.8–3.6 Å, respectively, due to π-stacking interactions between the aromatic imidazole rings. As shown in Figure 3 (b), the hexamers are connected by an unsupported Ag1–Ag1′ attraction [3.317(2) Å] and π-stacking interactions between the imidazole rings into a 1D Ag chain. The π-stacking interactions between the hexanuclear silver units are similar to those within the hexameric spiral. Other interactions in **2** are hydrogen bonds between lattice water molecules and uncoordinated nitrogen atoms, with separations between O and N of 2.722 (O1w–N10) and 2.728 Å (O2w–N6).

[Ag(μ-H_2biim)(nicotinate)]$_n$ (4)

Compound **4** has a monoanionic, organic counterion that is believed to account for the formation of an infinite helical structure (Figure 4), as in the case of **3** and [Ag(H_2-biim)]NO_3.[10b] Interestingly, unlike the nitrate analogue [Ag(H_2biim)]NO_3,[10b] **4** has the coordinating nitrogen atoms *trans* to each other, which leads to a considerably longer Ag···Ag separation (ca. 6 Å) than in **3** and [Ag(H_2-biim)]NO_3 (ca. 3 Å)[10b] due to the steric requirement of the bound nicotinate. This indicates that Ag–Ag attractions are not dominant in the Ag–H_2biim system. The Ag–$N_{nicotinate}$ distance [2.534(6) Å] is significantly longer than the Ag–N_{biim} distance [av. 2.188(5) Å]. The three N atoms around Ag^+ are approximately in a T-shaped arrangement with the N–Ag–N angles being 159.3°, 110.3° and 89.4°, respectively. The bridging H_2biim is twisted, with a dihedral angle of about 30°. The helices are held together through Ag···$O_{nicotinate}$ interactions (Ag1···O1 = 2.843, Ag1···O2 = 2.957 Å) and N–H···$O_{nicotinate}$ hydrogen bonds (N2···O1 = 2.689 Å) to form a sheet structure, as illustrated in Figure 5. The pyridyl rings of two nicotinate groups separated by about 3.6 Å are almost parallel to each other, which suggests significant π-stacking interactions.

Luminescent Properties

Metal complexes are promising luminescent materials for applications such as light-emitting materials owing to their ability to enhance, shift, and quench luminescent emission of organic ligands by metal coordination. Although numerous biimidazole complexes have been reported, their photophysical properties have been investigated only very re-

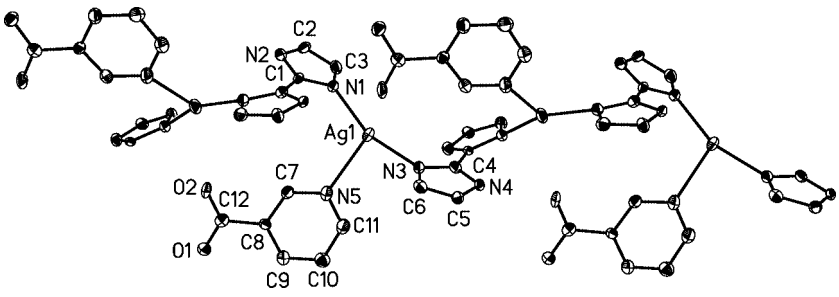

Figure 4. ORTEP drawing of [Ag(H_2biim)$_2$(nicotinate)]$_n$ (**4**) with 30% probability thermal ellipsoids.

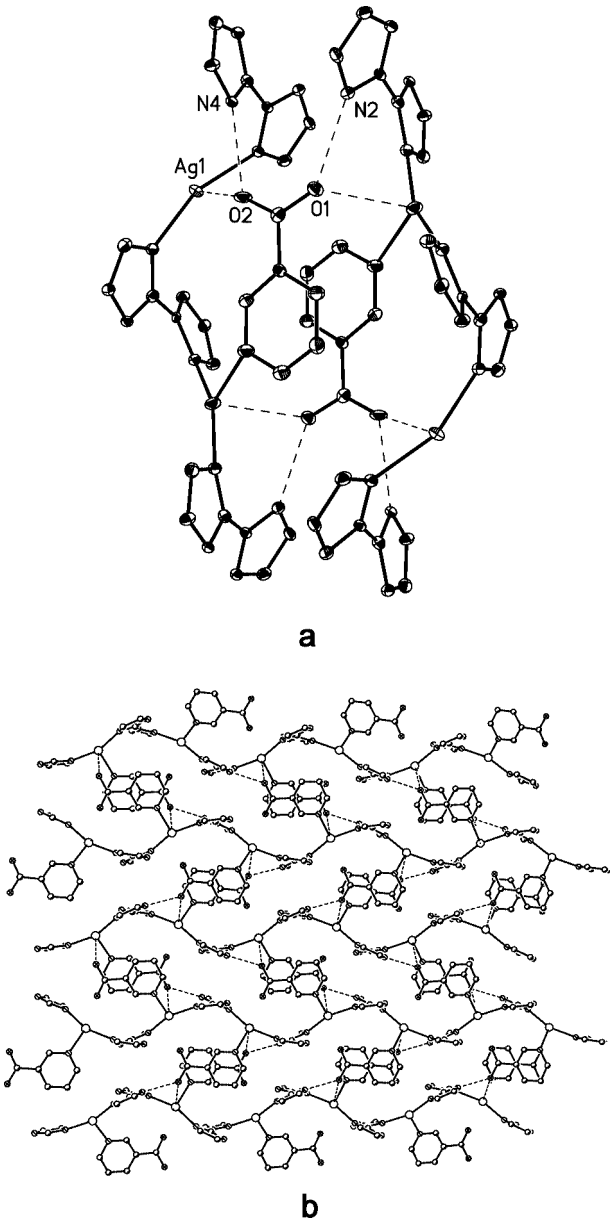

Figure 5. (a) Interhelix interactions and (b) multiple helices interconnected by nicotinate in **4**.

cently.[9a] The solid-state emission spectra of compounds **1**–**4** are shown in Figure 6. The free H_2biim ligand displays an emission maximum at 431 nm when excited at 334 nm in the solid state at ambient temperature. A violet-fluorescent emission band at 439 nm was observed for **1** upon excitation at 360 nm, attributable to the ligand-centered emission. Moreover, compound **1** exhibits violet-fluorescent emission bands at 346 nm and a yellowish-green radiation emission at lower energy (576 nm) upon excitation at 260 nm.

Upon excitation at a slightly longer wavelength (298 nm), compound **2** emits only one violet luminescence at 349 nm; the other one is probably quenched by oxalate. Excitation at 370 nm leads to greenish-blue photoluminescence with an emission maximum at 512 nm for **3**, similar to that in

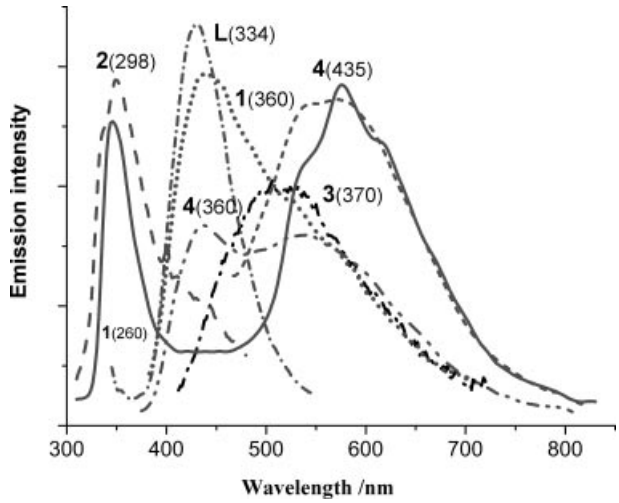

Figure 6. Luminescence emission spectra of **1**–**4** and **L** (H_2biim).

$[Ag(Me_2\text{-imy})_2][Ag\text{-}Cl_2]$ (544 nm), which possesses extended Ag–Ag interactions.[15] Compound **4** exhibits similar violet-fluorescent emission bands at 437 nm upon excitation at 360 nm. However, one more yellowish-green radiation emission of **4** was observed at 539 nm, presumably due to the aromatic nicotinate group. A similar yellowish-green fluorescent emission band at 571 nm was also observed for **4** upon excitation at 435 nm.

Conclusion

The structural topology of the Ag–H_2biim system is determined by the charge of the counteranions. Thus, dianionic counterions facilitate the formation of dimeric structures driven by the charge-balance requirement, whereas a monoanionic counterion favors the formation of helical structures. Larger counteranions lead to either finite helical structures or a *trans* arrangement of the coordinating nitrogen atoms because of steric requirements. Organic counteranions with a strong coordination ability bind to the Ag^+ ions while inorganic counteranions remain uncoordinated. The argentophilic attraction is not dominant in the Ag–H_2biim system. The fluorescence emission of H_2biim is effectively shifted upon coordination of the ligand to Ag^+.

Experimental Section

General Remarks: H_2biim was synthesized in accordance with a published procedure.[13] The reagents and solvents employed were commercially available and used as received without further purification. The C, H, and N microanalyses were carried out with a Vario EL III elemental analyzer. IR spectra were recorded with a Magna 750 FT-IR spectrometer photometer as KBr pellets in the range 4000–400 cm^{-1}. Fluorescent spectra were measured with an Edinburgh FLS920 analytical instrument.

***CAUTION**! Perchlorate salts are potentially explosive and should be handled with care and in small amounts.*

$[Ag_2(H_2biim)_2]SO_4 \cdot 2H_2O$ (1): Ag_2O (0.056 g, 0.25 mmol) was dissolved in 20 mL of aqueous H_2SO_4 (0.05 M) and H_2biim (0.067 g,

0.5 mmol) in 10 mL of aqueous H_2SO_4 (0.05 M) was added to the resulting solution. The mixture was stirred at room temperature for two hours, then the resulting solution was filtered off and the filtrate was left in air to evaporate to form crystals of **1** after a few days. The crystals were collected by filtration, washed with ethanol, and dried in air (0.114 g, 74% yield based on Ag). $C_{12}H_{16}Ag_2N_8O_6S$ (616.13): calcd. C 23.39, H 2.62, N 18.19; found C 23.34, H 2.70, N 18.12. IR (KBr): $\tilde{\nu}$ = 3446 m cm^{-1}, 3074 m, 3001 m, 2896 m, 2806 m, 1631 w, 1546 s, 1435 m, 1406 s, 1385 m, 1334 m, 1218 m, 1105 vs, 939 s, 886 s, 761 w, 747 m, 689 m, 617 m.

[Ag_2(H_2biim)$_2$(μ-ox)] (2): $AgNO_3$ (0.085 g, 0.5 mmol) was dissolved in 30 mL of H_2O and H_2biim (0.067 g, 0.5 mmol) was added to the resulting solution. The mixture was stirred at room temperature for

Table 1. Crystallographic data for compounds **1**–**4**.

Complex	**1**	**2**	**3**	**4**
Molecular formula	$C_{12}H_{16}Ag_2N_8O_6S$	$C_{14}H_{12}Ag_2N_8O_4$	$C_{46}H_{56}Ag_6Cl_4N_{28}O_{24}$	$C_{12}H_{10}AgN_5O_2$
Formula weight	616.13	572.06	2174.21	364.12
Crystal system	monoclinic	triclinic	monoclinic	monoclinic
Space group	*C*2/*c*	$P\bar{1}$	*C*2/*c*	*C*2/*c*
a [Å]	12.985(2)	7.5550(12)	25.857(17)	16.5276(6)
b [Å]	15.337(3)	7.8391(12)	14.424(8)	13.2996(5)
c [Å]	10.3207(17)	8.4408(13)	19.420(12)	12.0687(2)
α [°]	90	103.3800(10)	90	90
β [°]	113.440(3)	110.681(2)	114.698(6)	107.041(2)
γ [°]	90	105.975(2)	90	90
Volume [$Å^3$]	1885.8(5)	418.54(11)	6580(7)	2536.35(14)
Z	4	1	4	8
$d_{calcd.}$ [$g\,cm^{-3}$]	2.283	2.270	2.195	1.907
μ [cm^{-1}]	2.351	2.383	2.016	1.598
F(000)	1272	278	4280	1440
Crystal size [mm]	0.38 × 0.10 × 0.04	0.34 × 0.24 × 0.06	0.20 × 0.20 × 0.20	0.26 × 0.20 × 0.06
Data/restraint/parameters	1201/3/138	1440/0/127	5450/0/498	1777/0/181
Reflns. collected	2216	2195	18786	3223
Unique reflns.	1201	1440	5450	1777
Goodness of fit	1.134	1.582	1.206	1.390
$R_1[I > 2\sigma(I)]$	0.0545	0.0416	0.0506	0.0640
$\omega R_2[I>2\sigma(I)]$	0.1040	0.1203	0.0828	0.0886
R_1 (all data)	0.0812	0.0444	0.0685	0.0948
ωR_2(all data)	0.1133	0.1232	0.0893	0.0953
Residuals [$e\,Å^{-3}$]	0.507, –0.527	0.845, –1.079	1.363, –0.836	0.427, –0.587

Table 2. Selected bond lengths [Å] and angles [°] for **1**–**4**.[a]

Complex **1**					
Ag–N(1)	2.149(6)	Ag–N(3)	2.130(5)	Ag–Ag#1	2.8182(14)
N(3)–Ag–N(1)	170.6(2)	N(3)–Ag–Ag#1	87.55(17)	N(1)–Ag–Ag#1	84.85(16)
Complex **2**					
Ag–N(1)	2.236(4)	Ag–N(3)	2.203(4)	Ag–O(1)	2.392(4)
Ag–Ag#1	2.8437(9)	N(3)–Ag–N(1)	132.95(16)	N(3)–Ag–O(1)	131.28(14)
N(1)–Ag–O(1)	95.76(14)	N(1)–Ag–Ag#1	91.71(12)	N(3)–Ag–Ag#1	79.42(11)
O(1)–Ag–Ag#1	103.91(10)				
Complex **3**					
Ag(1)–N(1)	2.549(5)	Ag(1)–N(3)	2.163(5)	Ag(1)–N(5)	2.160(5)
Ag(1)–Ag(2)	2.9331(17)	Ag(1)–Ag(1)#1	3.3169(18)	Ag(2)–N(7)	2.139(5)
Ag(2)–N(11)	2.135(5)	Ag(2)–Ag(3)	3.0091(15)	Ag(3)–N(9)	2.111(5)
Ag(3)–N(13)	2.122(5)	Ag(3)–Ag(3)#2	3.0767(19)	N(3)–Ag(1)–N(1)	73.96(18)
N(5)–Ag(1)–N(1)	108.77(17)	N(5)–Ag(1)–N(3)	170.32(18)	N(3)–Ag(1)–Ag(2)	87.75(13)
N(5)–Ag(1)–Ag(2)	85.05(12)	N(1)–Ag(1)–Ag(2)	144.91(11)	N(5)–Ag(1)–Ag(1)#1	104.98(13)
N(3)–Ag(1)–Ag(1)#1	84.30(13)	N(1)–Ag(1)–Ag(1)#1	55.78(12)	Ag(2)–Ag(1)–Ag(1)#1	153.14(3)
N(11)–Ag(2)–N(7)	164.81(18)	N(11)–Ag(2)–Ag(1)	109.47(13)	N(7)–Ag(2)–Ag(1)	84.93(12)
N(11)–Ag(2)–Ag(3)	80.69(14)	N(7)–Ag(2)–Ag(3)	108.97(13)	Ag(1)–Ag(2)–Ag(3)	73.30(5)
N(9)–Ag(3)–N(13)	172.62(18)	N(9)–Ag(3)–Ag(2)	88.47(13)	N(13)–Ag(3)–Ag(2)	98.66(13)
N(9)–Ag(3)–Ag(3)#2	100.32(13)	N(13)–Ag(3)–Ag(3)#2	83.47(12)	Ag(2)–Ag(3)–Ag(3)#2	74.85(5)
Complex **4**					
Ag(1)–N(1)	2.260(16)	Ag(1)–N(3)	2.154(16)	Ag(1)–N(10)	2.301(14)
Ag(2)–N(5)	2.240(14)	Ag(2)–N(7)	2.172(12)	N(3)–Ag(1)–N(1)	157.7(6)
N(1)–Ag(1)–N(10)	111.8(5)	N(3)–Ag(1)–N(10)	90.3(6)	N(7)–Ag(2)–N(5)	161.0(5)

[a] Symmetry code for **1**: #1: –*x*, *y*, –*z* + 1/2; **2**: #1: –*x* + 1, –*y* + 1, –*z* + 2; **3**: #1: –*x* + 1/2, –*y* + 1/2, –*z* + 1; #2: –*x*, *y*, –*z* + 1/2.

half an hour then a water solution (20 mL) containing oxalic acid (0.032 g, 0.25 mmol) was added. The resulting solution was stirred at 80 °C for two hours and then filtered off. The filtrate was left in air to evaporate to form crystals of **2** after one day. The crystals were collected by filtration, washed with ethanol, and dried in air (0.093 g, 65% yield based on Ag). $C_{14}H_{12}Ag_2N_8O_4$ (572.06): calcd. C 29.39, H 2.12, N 19.59; found C 29.36, H 2.34, N 19.44. IR (KBr): $\tilde{\nu}$ = 3435 s cm^{-1}, 3142 w, 3076 m, 2999 m, 2898 m, 2807 m, 1597 s, 1545 s, 1435 w, 1406 s, 1384 m, 1334 w, 1310 s, 1218 w, 1105 s, 940 m, 886 m, 761 m, 747 m, 735 m, 689 m.

$[Ag_6(\mu\text{-}H_2biim)_5(H_2biim)_2](ClO_4)_4(CH_3CO_2)_2\cdot 4H_2O$ (3): An aqueous solution (10 mL) of $NaClO_4\cdot H_2O$ (0.70 g 0.5 mmol) was added to a well-stirred suspension of H_2biim (0.067 g, 0.5 mmol) and $Ag(CH_3COO)$ (0.083 g, 0.5 mmol) in 50 mL of water. The suspension was then refluxed for 2 h. After cooling, the resulting suspension was filtered off. The filtrate was left in air to evaporate the solvent and crystals were obtained after a few days. The product was collected by filtration, washed with ethanol, and dried in vacuo (0.078 g, 43% yield based on Ag). $C_{46}H_{56}Ag_6Cl_4N_{28}O_{24}$ (2174.2): calcd. C 25.41, H 2.60, N 18.04; found C 25.49, H 2.67, N 18.11. IR (KBr): $\tilde{\nu}$ = 3449 m cm^{-1}, 3176 w, 3143 w, 3076 m, 3002 m, 2898 m, 2807 m, 1631 w, 1546 m, 1436 w, 1406 m, 1384 s, 1333 m, 1218 w, 1144 m, 1121 s, 1106 s, 1084 s, 940 m, 887 m, 747 m, 689 m, 626 w.

$[Ag_2(H_2biim)_2(nicotinate)_2]_n$ (4): A mixture of $AgNO_3$ (0.042 g, 0.25 mmol), H_2biim (0.333 g, 0.25 mmol), and nicotinic acid (0.308 g, 0.25 mmol) in H_2O (16 mL) was heated at 165 °C for 3 d under autogenous pressure. After cooling, the resulting solution was filtered off. The filtrate was left in air to evaporate the solvent and crystals were obtained after a few days. The product was collected by filtration, washed with ethanol, and dried in vacuo (0.042 g, 46% yield based on Ag). $C_{12}H_{10}AgN_5O_2$ (364.12): calcd. C 39.58, H 2.77, N 19.24; found C 39.53, H 2.85, N 19.16. IR (KBr): $\tilde{\nu}$ = 3435 m cm^{-1}, 3109 m, 3067 m, 2991 m, 2896 m, 2806 m, 1594 s, 1547 s, 1406 m, 1384 s, 1334 m, 1219 w, 1191 w, 1152 w, 1105 m, 1030 w, 993 w, 940 w, 915 w, 774 m, 749 mw, 691 m.

Table 3. Hydrogen bonds in **1**–**4**.[a]

D–H···A	D–H	H···A	D–A	D–H–A
Complex **1**				
N2–H2A···O2#1	0.86	1.94	2.774	162.4
N4–H4A···O1#2	0.86	1.95	2.727	149.3
O1W–H1WB···O2#3	0.87	2.00	2.869	178.6
O1W–H1WA···O2#4	0.95	2.37	3.172	141.0
Complex **2**				
N2–H2A···O2#1	0.86	1.92	2.741	159.4
N4–H4B···O1#2	0.86	1.89	2.724	164.2
Complex **3**				
N2–H2A···O4#1	0.86	2.49	2.973	116.1
N2–H2A···O02	0.86	2.58	3.316	144.9
N4–H4A···O02	0.86	2.28	3.099	160.5
N4–H4A···O2#2	0.86	2.53	3.050	119.8
N6–H6A···O2W#3	0.86	1.89	2.726	174.9
N8–H8A···O02#4	0.86	2.36	3.078	140.9
N10–H10A···O1W	0.86	1.87	2.714	168.0
N12–H12A···O1W	0.86	2.34	3.017	135.4
N12–H12A···O7#5	0.86	2.35	2.927	125.2
N14–H14A···O01#6	0.86	1.87	2.722	172.7
O1W–H1WA···O2#2	0.90	2.16	2.840	132.2
O1W–H1WB···O01#7	0.90	1.96	2.796	153.9
O1W–H1WB···O5#5	0.90	2.56	3.067	116.3
O2W–H2WA···O02#8	0.91	2.19	3.034	153.3
O2W–H2WB···O01#7	0.90	2.52	3.147	127.0
Complex **4**				
N2–H1···O1#1	0.85	1.85	2.688	167.3
N4–H4···O2#2	0.93	1.80	2.694	161.0

[a] Symmetry codes for **1**: #1: $-x+1, -y+1, -z+1$; #2: $-x+1, -y, -z+1$; #3: $x, y, z-1$; #4: $-x+1/2, -y+1/2, -z+1$; **2**: #1: $x+1, y+1, z$; #2: $x, y, z+1$; **3**: #1: $x, -y+1, z+1/2$; #2: $-x+1/2, y+1/2, -z+1/2$; #3: $x, y-1, z$; #4: $-x+1/2, -y+1/2, -z+1$; #5: $x, -y+1, z-1/2$; #6: $x-1, y-1, z$; #7: $-x+1, y, -z+1/2$; #8: $-x+1/2, -y+3/2, -z+1$. **4**: #1: $-x+1/2, y-1/2, -z+3/2$; #2: $x, y, z-1$.

X-ray Crystallographic Study: Suitable single crystals of complexes **1**–**4** were mounted on a Siemens Smart CCD diffractometer equipped with a graphite-monochromated Mo-K_α radiation source (λ = 0.71073 Å) at 298 K. All absorption corrections were performed with the SADABS program. All structures were solved by direct methods and refined by full-matrix least-squares fitting on F^2 with SHELXTL-97.[14] All non-hydrogen atoms were refined with anisotropic thermal parameters. Hydrogen atoms were located at geometrically calculated positions and treated as riding on their parent atoms. Crystallographic data and structural refinements for compounds **1**–**4** are summarized in Table 1. Selected bond lengths and hydrogen bonds are summarized in Tables 2 and 3, respectively. CCDC-285100 (**1**), -285101 (for **2**), -262860 (for **3**), and -285012 (for **4**) contain the supplementary crystallographic data for this paper. These data can be obtained free of charge from The Cambridge Crystallographic Data Center via www.ccdc.cam.ac.uk/data_request/cif.

Acknowledgments

This work was supported by the National Science Foundation of China (grant no. 20473092) and the "One Hundred Talents Program" of the Chinese Academy of Science.

[1] a) *Comprehensive Supramolecular Chemistry* (Eds.: J. L. Atwood, J. E. D. Davies, J. M. Lehn, D. D. MacNicol, F. Vögtle), Pergamon, Oxford, **1996**; b) J.-M. Lehn, *Supramolecular Chemistry − Concepts and Perspectives*, VCH, Weinheim, **1995**.

[2] a) D. Philp, J. F. Stoddart, *Angew. Chem. Int. Ed. Engl.* **1996**, *35*, 1155–1196; b) O. M. Yaghi, H. Li, C. Davis, D. Richardson, T. L. Groy, *Acc. Chem. Res.* **1998**, *31*, 474–484; c) S. R. Batten, R. Robson, *Angew. Chem. Int. Ed.* **1998**, *37*, 1460–1494.

[3] a) S. Leininger, B. Olenyuk, P. J. Stang, *Chem. Rev.* **2000**, *100*, 853–891; b) M. Fujita, *Acc. Chem. Res.* **1999**, *32*, 53–61.

[4] a) P. Pyykkö, *Chem. Rev.* **1997**, *97*, 597–636; b) P. Pyykko, F. Mendizabal, *Chem. Eur. J.* **1997**, *3*, 1458–1465.

[5] a) P. Majumdar, K. K. Kamar, A. Castiñeiras, S. Goswami, *Chem. Commun.* **2001**, 1292–1293; b) V. J. Catalano, S. J. Horner, *Inorg. Chem.* **2003**, *42*, 8430–8438; c) E. J. Fernandez, J. M. Lopez de Luzuriaga, M. Monge, M. A. Rodriquez, O. Crespo, M. Concepcion, A. Laguna, P. G. Jones, *Inorg. Chem.* **1998**, *37*, 6002–6008; d) M. Munakata, M. Maekawa, S. Kitagawa, M. Adachi, H. Masuda, *Inorg. Chim. Acta* **1990**, *167*, 181–188.

[6] a) A. N. Khlobystov, A. J. Blake, N. R. Champness, D. A. Lemenovskii, A. G. Majouga, N. V. Zyk, M. Schroder, *Coord. Chem. Rev.* **2001**, *222*, 155–192; b) M. A. Withersby, A. J. Blake, N. R. Champness, P. Hubberstey, W. S. Li, M. Schroder, *Angew. Chem. Int. Ed. Engl.* **1997**, *36*, 2327–2329.

[7] a) M. J. Hannon, C. L. Painting, E. A. Plummer, L. J. Childs, N. W. Alco, *Chem. Eur. J.* **2002**, *8*, 2225–2238; b) S. Lopez, S. W. Keller, *Inorg. Chem.* **1999**, *38*, 1883–1888; c) K. A. Hirsch, S. R. Wilson, J. S. Moore, *Inorg. Chem.* **1997**, *36*, 2960–2968.

[8] a) B. Hasenknopf, J. M. Lehn, N. Boumediene, A. Dupont-Gervais, A. Van Dorsselaer, B. O. Kneisel, D. Fenske, *J. Am.*

Chem. Soc. **1997**, *119*, 10956–10962; b) R. D. Schnebeck, E. Freisinger, B. Lippert, *Angew. Chem. Int. Ed.* **1999**, *38*, 168–171; c) D. A. Mcmorran, P. J. Steel, *Angew. Chem. Int. Ed.* **1998**, *37*, 3295–3297; d) J. S. Fleming, K. L. V. Mann, C. A. Carraz, E. Psillakis, J. C. Jeffery, J. A. McCleverty, M. D. Ward, *Angew. Chem. Int. Ed.* **1998**, *37*, 1279–1281; e) P. C. Jones, K. J. Byrom, J. C. Jeffery, J. A. McCleverty, M. D. Ward, *Chem. Commun.* **1997**, 1361–1362.

[9] a) R.-L. Sang, L. Xu, *Inorg. Chem.* **2005**, *44*, 3731–3737; b) M. Tadokoro, K. Isober, H. Uekusa, Y. Ohashi, J. Toyoda, K. Tashiro, K. Nakasuji, *Angew. Chem. Int. Ed.* **1999**, *38*, 95–98; c) M. Tadocoro, H. Kanno, T. Kitajima, H. Shimada-Umemoto, N. Nakanishi, K. Isobe, K. Nakasuji, *Proc. Natl. Acad. Sci. USA* **2002**, *99*, 4950–4955; d) M. Tadocomo, T. Shiomi, K. Isobe, K. Nakasuji, *Inorg. Chem.* **2001**, *40*, 5476–5478; e) M. Tadomoro, K. Nakasuji, *Coord. Chem. Rev.* **2000**, *198*, 205–218; f) R. Atencio, M. Chacon, T. Gonzalez, A. Briceno, G. Agrifoglio, A. Sierraalta, *Dalton Trans.* **2004**, 505–513; g) W. E. Allen, C. J. Fowler, V. M. Lynch, J. L. Sessler, *Chem. Eur. J.* **2001**, *7*, 721–729; h) L. Ohrstrom, K. Larsson, S. Borg, S. T. Norberg, *Chem. Eur. J.* **2001**, *7*, 4805–4810.

[10] a) C. Kirchner, B. Krebs, *Inorg. Chem.* **1987**, *26*, 3569–3576; b) C. A. Hester, R. G. Baughman, H. L. Collier, *Polyhedron* **1997**, *16*, 2893–2895; c) A. S. Abushamleh, H. A. Goodwin, *Aust. J. Chem.* **1979**, *32*, 513–518; d) U. Sakaguchi, A. K. Addison, *J. Chem. Soc., Dalton Trans.* **1979**, 600–608; e) A. Bendini, F. Mani, *Inorg. Chim. Acta* **1988**, *154*, 215–219; f) S. Fortin, A. L. Beauchamp, *Inorg. Chem.* **2000**, *39*, 4886–4893; g) M. A. Lorente, F. Dahan, Y. Sanakis, V. Petrouleas, A. Boussedsou, J.-P. Tuchagues, *Inorg. Chem.* **1995**, *34*, 5346–5357; h) I. G. Dance, A. S. Abushamleh, H. A. Goodwin, *Inorg. Chim. Acta* **1980**, *43*, 217–221; i) A. D. Mighell, C. W. Reimann, F. A. Maucer, *Acta Crystallogr., Sect. B* **1969**, *25*, 60–66; j) J. Cancela, M. J. Gonzalez Garmendia, M. Qurios, *Inorg. Chim. Acta* **2001**, *313*, 156–159; k) B.-H. Ye, F. Xue, G.-Q. Xue, L.-N. Ji, T. C. W. Mak, *Polyhedron* **1999**, *18*, 1785–1790; l) R.-L. Sang, L. Xu, *Acta Crystallogr., Sect. E* **2005**, *61*, m793–m795.

[11] a) S. W. Kaiser, R. B. Saillant, W. M. Butler, P. G. Rasmussen, *Inorg. Chem.* **1976**, *15*, 2681–2687; b) S. W. Kaiser, R. B. Saillant, P. G. Rasmussen, *J. Am. Chem. Soc.* **1975**, *97*, 425–426; c) S. W. Kaiser, R. B. Saillant, W. M. Butler, P. G. Rasmussen, *Inorg. Chem.* **1976**, *15*, 2688–2694; d) M. S. Haddad, D. N. Hendrickson, *Inorg. Chem.* **1978**, *17*, 2622–2630; e) R. Usón, J. Gimeno, J. Forniés, F. Martínez, *Inorg. Chim. Acta* **1981**, *50*, 173–177; f) A. Maiboroda, G. Rheinwald, H. Lang, *Inorg. Chem. Commun.* **2001**, *4*, 381–383; g) P. Majumdar, S. M. Peng, S. Goswami, *J. Chem. Soc., Dalton Trans.* **1998**, 1569–1574; h) M. P. Garcia, A. M. López, M. A. Esteruelas, F. J. Lahoz, L. A. Oro, *J. Chem. Soc., Chem. Commun.* **1988**, 793 –795; i) R. Usón, L. A. Oro, J. Gimeno, M. A. Ciriano, J. A. Cabeza, *J. Chem. Soc., Dalton Trans.* **1983**, 233–330.

[12] a) J.-S. Casas, A. Castineiras, Y. Parajo, M.-L. Perez-Paralle, A. Sanchez, A. Sanchez-Gonzalez, J. Sordo, *Polyhedron* **2003**, *22*, 1113–1121; b) A. Sanchez-Gonzalez, J. S. Casas, J. Sordo, U. Russo, M. I. Lareo, B. J. Regueiro, *J. Inorg. Biochem.* **1990**, *39*, 227–235; c) C. Lopez, A. S. Gonzalez, M. E. Garcia, J. S. Casas, J. Sordo, R. Graziani, U. Casellato, *J. Organomet. Chem.* **1992**, *434*, 261–268; d) B. J. Holliday, C. A. Mirkin, *Angew. Chem. Int. Ed.* **2001**, *40*, 2023–2043; e) J. D. Watson, F. H. C. Crick, *Nature* **1953**, *171*, 737–738; f) P. A. Zoo, J. S. Casas, M. D. Couse, E. Freijanes, A. Furlani, V. Scarcial, J. Sordo, U. Russo, M. Varela, *Appl. Organomet. Chem.* **1997**, *11*, 963–968.

[13] R. P. Thummel, V. Goulle, B. Chen, *J. Org. Chem.* **1989**, *54*, 3057–3061.

[14] G. M. Sheldrick, *SHELXL-97, Program for Crystal Structure Solution*, University of Göttingen, Germany, **1997**.

[15] K. M. Lee, H. M. J. Wang, I. J. B. Lin, *J. Chem. Soc., Dalton Trans.* **2002**, 2852–2856.

Received: October 1, 2005
Published Online: February 2, 2006

